Design, synthesis and biological evaluation of novel scaffold benzo[4,5]imidazo [1,2-*a*]pyrazin-1-amine: towards adenosine A_{2A} receptor (A_{2A} AR) antagonist

G. Lakshma Reddy, Rupam Sarma, Shuhao Liu, Weifeng Huang, Jinping Lei, Jiasheng Fu, Wenhao Hu

PII: S0223-5234(20)31012-6

DOI: https://doi.org/10.1016/j.ejmech.2020.113040

Reference: EJMECH 113040

To appear in: *European Journal of Medicinal Chemistry*

Received Date: 6 March 2020

Revised Date: 11 November 2020

Accepted Date: 14 November 2020

Please cite this article as: G.L. Reddy, R. Sarma, S. Liu, W. Huang, J. Lei, J. Fu, W. Hu, Design, synthesis and biological evaluation of novel scaffold benzo[4,5]imidazo [1,2-*a*]pyrazin-1-amine: towards adenosine A_{2A} receptor (A_{2A} AR) antagonist, *European Journal of Medicinal Chemistry*, https://doi.org/10.1016/j.ejmech.2020.113040.

Graphical Abstract

Design, synthesis and biological evaluation of novel scaffold benzo[4,5]imidazo[1,2-*a*]pyrazin-1-amine: towards adenosine A_{2A} receptor (A_{2A} AR) antagonist

G. Lakshma Reddy, Rupam Sarma, Shuhao Liu, Weifeng Huang, Jinping Lei,* Jiasheng Fu,* Wenhao Hu*

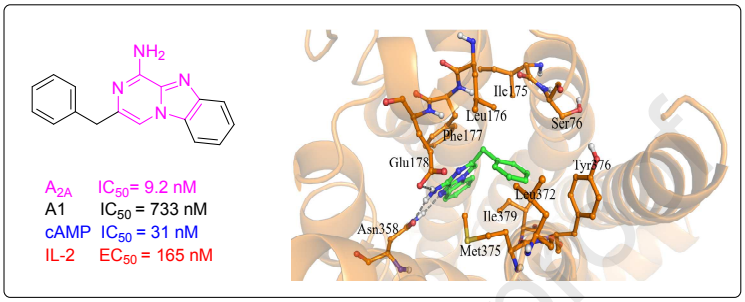

Design, synthesis and biological evaluation of novel scaffold benzo[4,5]imidazo [1,2-*a*]pyrazin-1-amine: towards adenosine A_{2A} receptor (A_{2A} AR) antagonist

G. Lakshma Reddy,[a#] Rupam Sarma,[a,b#] Shuhao Liu,[a] Weifeng Huang,[a] Jinping Lei,*[,a] Jiasheng Fu,*[,a] Wenhao Hu*[,a]

[a] *Guangdong Key Laboratory of Chiral Molecule and Drug Discovery, School of Pharmaceutical Sciences, Sun Yat-Sen University, Guangzhou 510006, China*
[b]*Department of Chemistry, Nalbari College, Assam 781335, India.*

#Authors contributed equally to this work

**Corresponding author*

E-mail: huwh9@mail.sysu.edu.cn

Abstract:

Antagonists of adenosine receptor are under exploration as potential drug candidates for treatment of neurological disorders, depression, certain cancers and potentially used as a cancer immunotherapy. Herein, we describe design and synthesis of novel scaffold benzo[4,5]imidazo [1,2-*a*]pyrazin-1-amine (**6**) derivatives. All the compounds were evaluated for A_{2A} AR antagonist activity and displayed encouraging results (IC_{50} 9 to 300 nM) of A_{2A} AR antagonist binding affinity in biochemical assay. Compound **27** exhibits good activity in A_{2A} AR antagonist cAMP functional assay (IC_{50} 31 nM) and further this compound shows T-cell activation at the IL-2 production assay (EC_{50} 165 nM). Molecular docking studies were carried out to rationalize the observed binding affinity of compound **27**.

Keywords: Benzo[4,5]imidazo[1,2-*a*]pyrazin-1-amine, Adenosine A_{2A} receptor (A_{2A} AR) antagonist, T-Cell activation, cancer immunotherapy.

1. Introduction

Adenosine, a naturally occurring nucleoside is present in all tissues of mammalian organisms. Extracellular adenosine modulates a wide range of physiological processes through interacting with cell surface adenosine receptors (ARs) which belong to a super family of G protein coupled receptors (GPCRs) having seven transmembrane helices.[1] There are four subtypes of AR (A_1, A_{2A}, A_{2B}, and A_3) which differ in size (A_1, A_{2B}, A_3 and A_{2A} consist of 326, 328, 318 and 409 amino acids, respectively), exhibit unique tissue distributions.[2] While A_1, A_{2A}, and A_3 receptors show high affinity, A_{2B} receptor has low affinity for adenosine binding.[3] Among these A_{2A} and A_{2B}, ARs increase the intracellular second messenger 3′,5′-cyclic adenosine monophosphate (cAMP) levels by coupling to G_s (A_{2A}), G_s /G_q (A_{2B}), whereas the A_1 and A_3 AR subtypes decreases intracellular cAMP levels *via* activation of G_i /G_o (A_1) and G_i /G_q (A_3).[4] In humans, the A_{2A} adenosine receptors have been expressed in a huge array of organs and tissues, including heart, lung, liver, cardiovascular tissues, neutrophils, leukocytes, and endothelial cells with remarkable implications in the regulation of inflammatory and immune responses.[5,6] On account of these reasons, there is a growing interest in the A_{2A} AR as a drug target.[5,7,8] Agonists are explored as anti-inflammatory agents[5,9-12] and antagonists have emerged as an attractive target to treat neurodegenerative diseases (Parkinson's disease, Huntington's, and Alzheimer's disease),[13-16] as well as in cancer immunotherapy.[3,8,17] A_{2A} ARs are widely expressed in several immune cell types: T cells, natural killer T (NLT) cells, dendritic cells (DCs), monocytes and natural killer cells (NK).[3,17] In tumor microenvironment (TME) augmentation in extracellular adenosine level enhances the signals of A_{2A} AR present on immune cells. Activation of A_{2A} AR on T cells and NK cells causes immunosuppression by reducing their proliferation, maturation, cytokine production (IL-2, IFN-γ) and tumor killing activity.[17-19] Recent studies have highlighted/supported[7,20] that A_{2A} AR knock out or use of A_{2A} AR antagonist in animal model has exhibited potent effects in increasing anti-tumor immunity and suppresses tumor growth.[21-24]

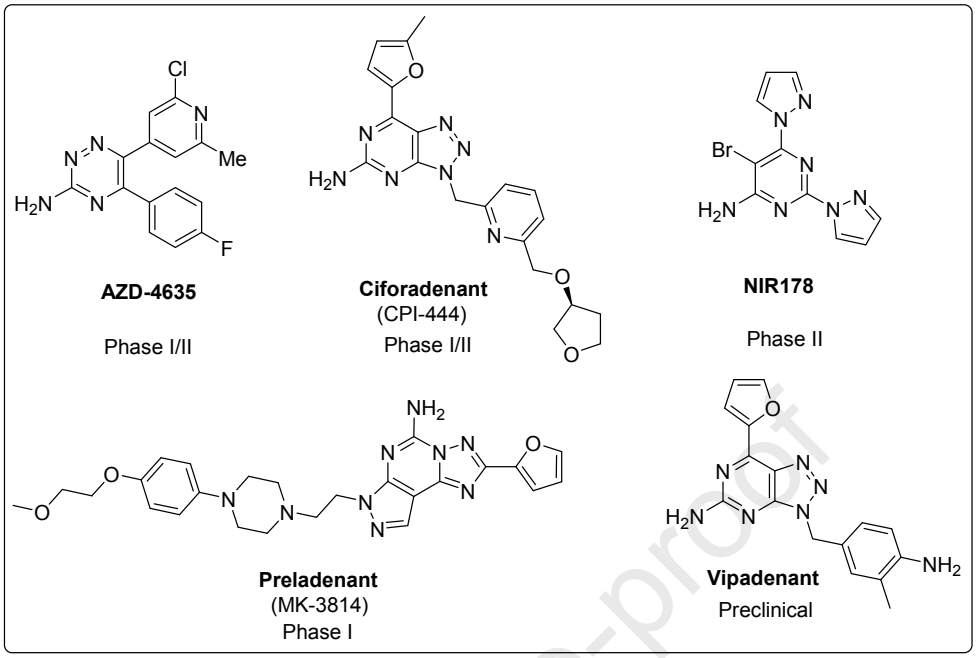

Fig. 1. A_{2A} AR antagonist candidates in clinical trials for cancer immunotherapy.

Currently some A_{2A} AR antagonists are in clinical trial for cancer immunotherapy either alone or in combination with other immunotherapies (Fig 1).[25-27]

2. Design

Owing to our interest in adenosine receptors, we approached to design and synthesize novel A_{2A} receptor antagonists based on the structures reported in literatures. Recently Falsini M. *et al* and Poli et al reported 1,2,4-triazolo[4,3-*a*] pyrazin-3-one (**1** and **2**) and imidazo[1,2-*a*]pyrazin-8-amine (**3**) derivatives respectively as adenosine A_{2A} R antagonists.[28-30] Similarly G. Yao and H. Peng *et al* reported 1,2,4-triazolo[1,5-*c*]pyrimidin-5-amine derivatives (**4** and **5**).[31,32] Taking the advantage of these bicyclic scaffolds, we designed novel structurally diversified tricyclic benzo[4,5] imidazo[1,2-*a*] pyrazin-1-amine (**6**) core structure (Fig 2) to investigate the antagonism of its derivatives in the adenosine A_{2A} AR pathway.

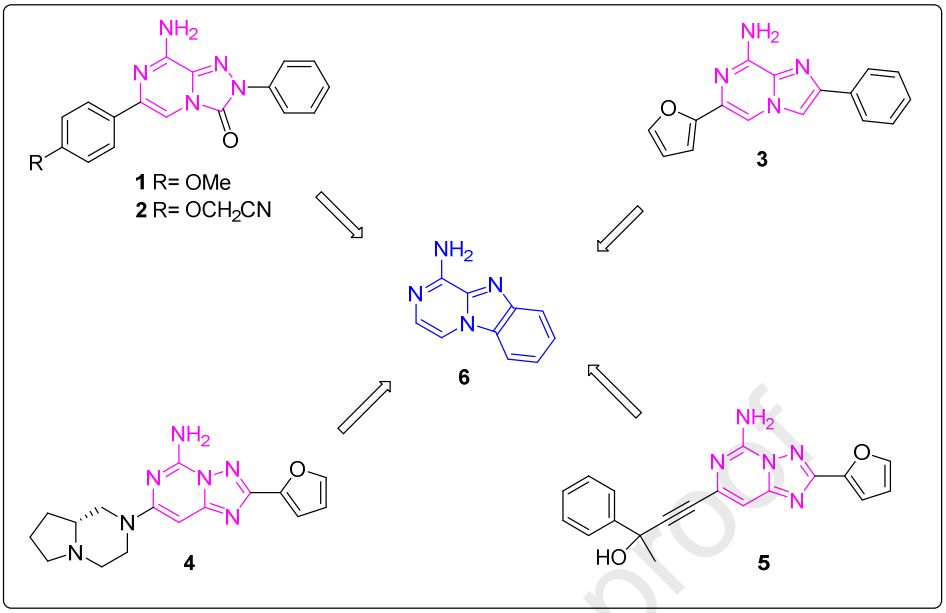

Fig. 2. Design of benzo[4,5] imidazo[1,2-*a*]pyrazin-1-amine scaffold.

3. Results and Discussion

3.1. Chemistry

Synthesis of imidazo[1,2-*a*]pyrazine has been reported in literature.[33] However, to the best of our knowledge no synthetic chemistry has been reported to construct benzo[4,5]imidazo[1,2-*a]*pyrazin-1-amine. We designed our synthetic strategy from *o*-phenylenediamine (**7**) to achieve the target products in four steps (Scheme 1). *o*-Phenylenediamine was treated with methyl 2,2,2-trichloroacetimidate in AcOH to give intermediate **8** in 87 % yield[34] which was further treated with ammonia solution to yield the corresponding 1*H*-benzo[*d*]imidazole-2-carbonitrile (**9**) in 83% yield.[35] Subsequently *N*-alkylation of **9** and **6** with the corresponding α-haloketones in different solvents such as DMF, DCM and CH_3CN, in the presence of variety of bases furnished the precursor intermediate 1-(2-oxo-2-phenylethyl)-1*H*-benzo[*d*]imidazole-2-carbonitrile (**10a-10s**). Recently we have optimized the cyclization condition for the formation of target compounds and the methodology is ready to publish in another manuscript. As a matter of interest we are here, showing only the optimized condition for this cyclization reaction. Treatment of compound **10** with ammonium acetate in acetic acid resulted in the target compounds (**11-17, 19-30)** in moderate to good yield (Table 1). Treatment of compound **17** with BBr_3 in DCM (Scheme 1) provided target compound **18** (Table 1).

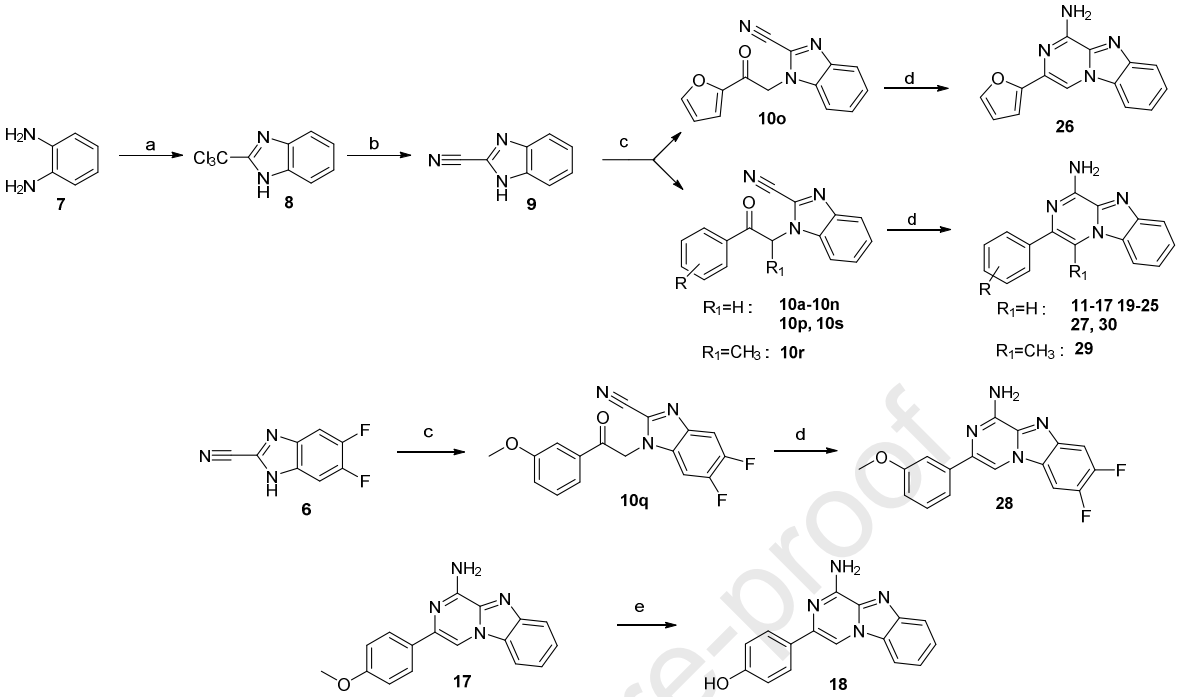

Scheme 1. Reagents and conditions: a) methyl 2,2,2-trichloroacetimidate, AcOH, rt, 87%. b) 0 ± 0.4M) NH_3 in dioxane and (7.0 M) NH_3 in MeOH, sealed tube, 0 ^oC to rt, 83%. c) $RCOCH_2X$, base, solvent. d) NH_4OAc, AcOH, sealed tube 90 ^oC. e) BBr_3, DCM, N_2, 0 ^oC to rt, 50%.

Table 1. Synthesized compounds based on Benzo[4,5]imidazo[1,2-*a*]pyrazin-1-amine scaffold.

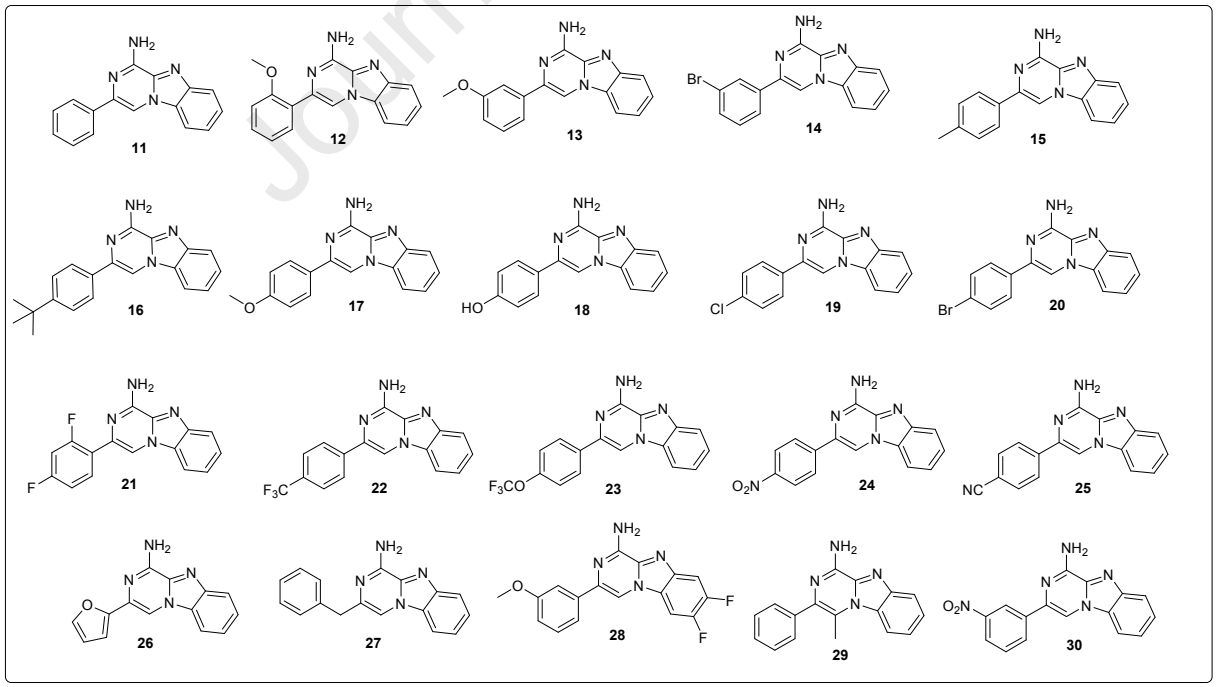

Further, compounds **24** and **30** were modified to obtain *N*-acetylated compounds **37** and **38** for the screening purpose (**Scheme 2)**. First, protection of amine group as di-Boc (**31**/**32**) by treating **24** or **30** with Boc_2O was performed. Nitro group was then reduced to amine with H_2 in the presence of Pd/C in methanol at room temperature, followed by acylation furnished the intermediate (**35**/**36**). Di-Boc was removed with TFA to yield the target compounds **37** and **38** in 50% and 57% yield respectively.

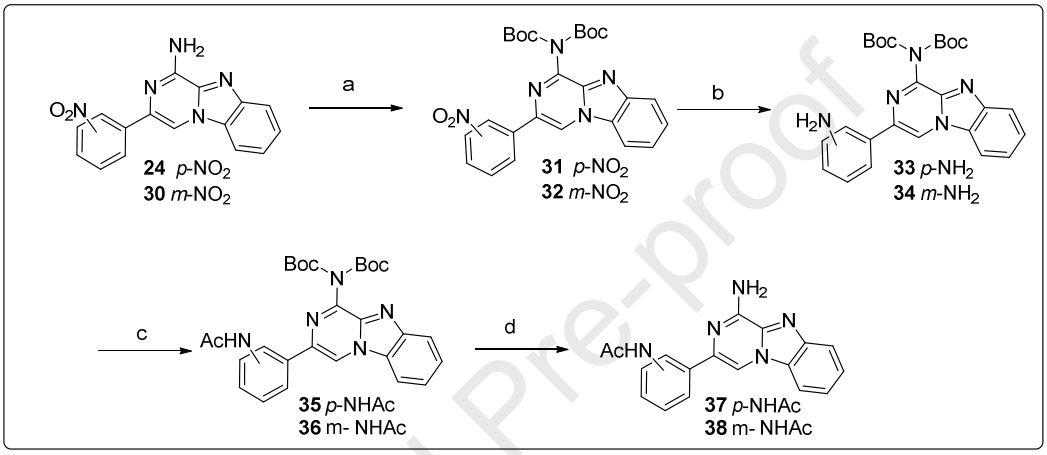

Scheme 2. Reagents and conditions: a) Boc_2O, TEA, DMAP, THF, 0 ^oC to rt, 70% b) H_2, 10% Pd/C, MeOH, r.t. c) Ac_2O, TEA, DMAP, DCM, 0 ^oC to rt, two steps 50% d) TFA, DCM 0 ^oC to rt, 50-57%.

To study the effect of aliphatic substituents on the A_{2A} AR binding affinity we synthesized compounds **43**, **44** and **45** (Scheme 3)**.** The synthesis was commenced by α-bromination of *tert*-butyl 4-acetylpiperidine-1-carboxylate (**39**) using Br_2, offered intermediate **40** in 74% yield, which was further used for *N*-alkylation on 1*H*-benzo[*d*]imidazole-2-carbonitrile to give intermediate **41** in 66% yield. Cyclization of **41** in the presence of ammonium acetate furnished compound **42** in 70% yield. Compound **42** was treated with TFA in DCM to obtain **43** in 60% yield and alkylation was done using different alkyl halides to obtain compound **44** and **45** in 30% and 43% yield respectively.

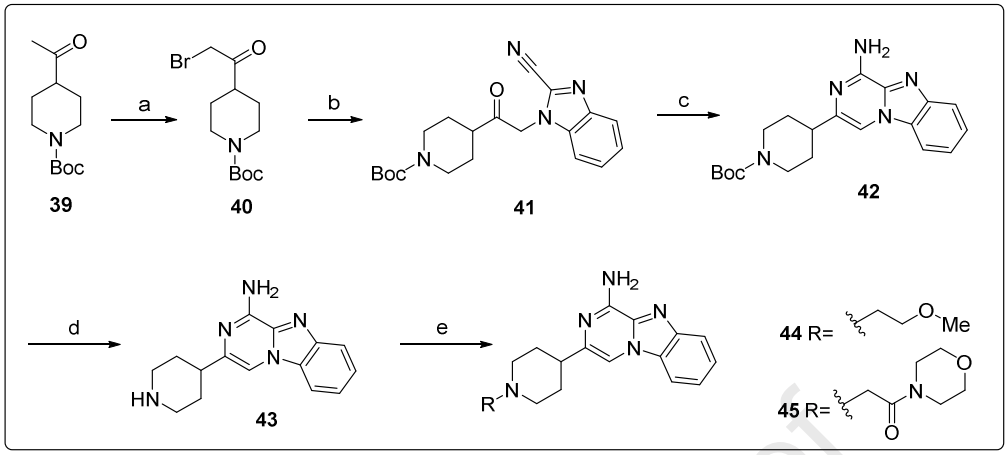

Scheme 3. Reagents and conditions: a) LHMDS, TMSCl, Br_2, THF, -78 to 0 ^oC, 74% b) **9**, K_2CO_3, DMF, 0 ^oC to rt, 66% c) NH_4OAc, AcOH, sealed tube, 90 ^oC 70% d)TFA, DCM 0 ^oC to rt, 60 % e) RX, K_2CO_3, DMF 0 ^oC to rt, **44** and **45** in 30% and 43%.

The synthesis of compound **50** (**Scheme 4)** started from 3-bromoprop-1-yne (**46**), which was treated with (diacetoxyiodo)benzene in acetonitrile at room temperature to provide **47** in 45% yield. Intermediate **47** was used for *N*-alkylation on 1*H*-benzo[*d*]imidazole-2-carbonitrile afforded intermediate **48** in 70% yield. Cyclization of **48** with ammonium acetate in acetic acid furnished compound **49** in 70% yield, which was further hydrolyzed to offer compound **50** in 60% yield.

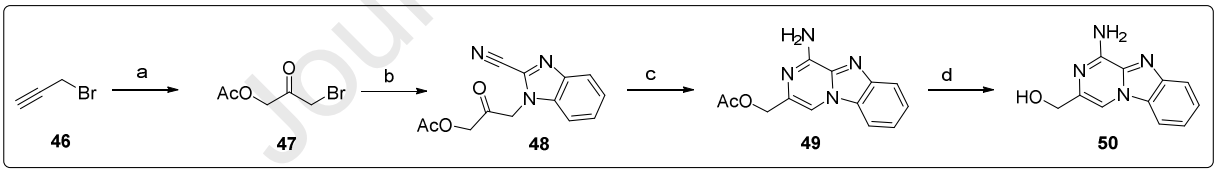

Scheme 4. Reagents and conditions: a) $PhI(OAc)_2$, AgOAc, H_2O, ACN, rt, 45% b) **9**, DIPEA, ACN, - 20 ^oC, 70% c) NH_4OAc, AcOH, sealed tube, 90 ^oC 70% d) K_2CO_3, MeOH, 0 ^oC to rt 60%.

3.2. Biology studies

3.2.1. A_{2A} AR binding assay

The biological activity of the synthesized benzo[4,5]imidazo[1,2-*a*]pyrazin-1-amine derivatives toward hA_{2A} receptor were first evaluated in an *in-vitro* receptor binding assay. Competitive binding experiments were performed using membrane preparation of the human recombinant A_{2A} AR overexpressed from HEK-293 cells and [^{3}H]-ZM241385 was used as a radioligand. The binding data of synthesized compounds are listed in Table 2.

Sensible activity was observed for compound **11** comparable to its analogue compound **12** with an *ortho*-OMe substituent. Encouraging results were obtained for *meta*-substituted -OMe, -Br and -NHAc compounds (Table 2, compound **13, 14** and **38**). In continuation *para*-position of the ring was also analyzed with various electron donating and withdrawing groups. Although the weakly electron donating groups such as methyl and *tert*-butyl groups were found to be promising (Table 2, compound **15** and **16**) yet same was not noticed in case of the moderate to strong electron donating groups such as -NHAc, -OMe, and –OH (Table 2, compound **37**, **17**, **18**). Halo substituted analogues chloro, bromo, 2,6 di-fluoro–CF_3 and –OCF_3 analogues demonstrated moderate to inferior results (Table 2, compound **19**, **20**, **21**, **22** and **23**). Electron withdrawing groups such as cyano and nitro showed lower activity compared with unsubstituted analogue (Table 2, compound **24** and **25**).

Table 2. Binding affinity data IC_{50} (nM) for compounds against human adenosine A_{2A} receptors[a].

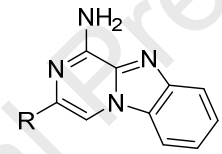

Comp	R	hA_{2A} (nM)	Comp	R	hA_{2A} (nM)
11	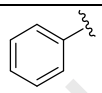	46.50 ± 0.98	**24**	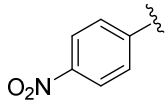	71.90 ± 0.90
12	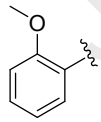	83.10 ± 0.99	**25**	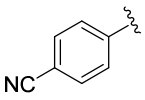	74.40 ± 0.96
13	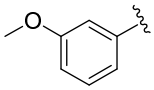	10.10 ± 0.96	**26**		32.60 ± 0.97
14	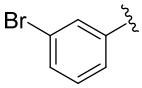	10.10 ± 0.98	**27**	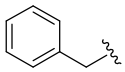	9.20 ± 0.97
15	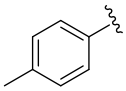	14.40 ± 0.99	**37**	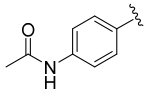	311.80 ± 0.83
16	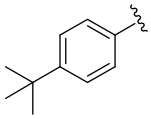	33.00 ± 0.95	**38**	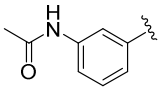	48.60 ± 0.97
17	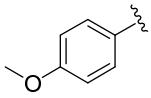	51.20 ± 0.96	**43**	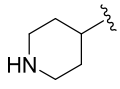	>10000

18	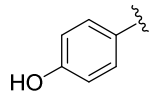	81.30 ± 0.95	**44**	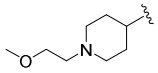	>10000
19	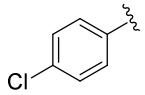	35.40 ± 0.98	**45**	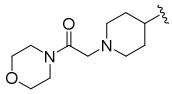	>10000
20	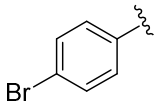	38.40 ± 0.97	**50**	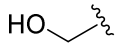	149.00 ± 0.88
21	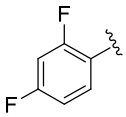	33.70 ± 0.94	**28**	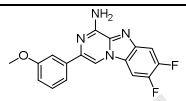	27.00 ± 0.99
22	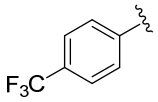	26.50 ± 0.92	**29**	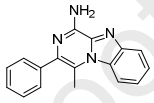	113.70 ± 0.84
23	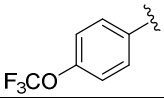	130.80 ± 0.98			

[a]Data are expressed as means ± SEM.

The aryl heterocyclic furan analogue (Table 2, compound **26**) displayed comparable $A_{2A}R$ binding as phenyl compound. However, heterocyclic piperidine and *N*-substituted piperidine at 3-position revealed slumped activity (Table 2, compound **43**, **44** and **45**). Replacement of the phenyl ring at 3-position by CH_2OH group further reduced the activity (Table 2 compound **50**). It has been noticed that the activity was further suppressed by introducing methyl group at 4-position of benzo[4,5]imidazo [1,2-*a]*pyrazin-1-amine (Table 2 compound **29**). Interestingly it was observed that when aryl was replaced with benzyl (on carbon atom spacer) moiety, 5-fold increased $A_{2A}R$ binding affinity (Table 2, compound **27**) was observed compared with phenyl analogue (Table 2, compound **11**).

3.2.2. A_1 AR binding assay

While all of the synthesized compounds were screened for A_{2A} binding affinity, a few potent A_{2A} binders were selected for the selectivity evaluation against human A_1 adenosine receptor. *In-vitro* competitive binding experiments with the hA_1 CHO-K1 membranes were performed using [^{3}H] DPCPX as a radioligand. Among all the compounds screened, *p*-tolyl (**15**), 3-bromophenyl (**14**), 3-methoxyphenyl (**13**) and 7,8-difluoro-3-(3-methoxyphenyl) (**28)** showed low selectivity of A_{2A} AR to A_1 AR, however the A_{2A} binding affinity of benzyl substituted analogue (**27**) was 80-fold more potent than A_1. Interestingly, the analogues with furan-2-yl (**26**), 3-acetamidophenyl (**38**) and 2,4-difluorophenyl (**21**) displayed higher binding affinity to A_1 AR than to A_{2A} AR.

Table 3. Binding affinity data for selected compounds against human adenosine A_{2A} and A_1 receptors[a].

Compound	hA_{2A} IC_{50} (nM)	A_1 IC_{50} (nM)	A_1/A_{2A}
13	10.10 ± 0.96	95.80 ± 0.96	9.5
14	10.10 ± 0.98	92.10 ± 0.98	9.1
15	14.40 ± 0.99	63.90 ± 0.92	4.4
21	33.70 ± 0.94	4.40 ± 0.93	0.13
26	32.30 ± 0.97	6.30 ± 0.98	0.20
27	9.20 ± 0.97	733.40 ± 0.97	79.7
28	27.00 ± 0.99	460.30 ± 0.99	17.0
38	48.60 ± 0.97	17.00 ± 0.87	0.35

[a]Data are expressed as means ± SEM.

3.2.3. cAMP functional assay

Over-activation of A_{2A} AR signal in tumor microenviroment triggers the accumulation of intracellular cAMP through stimulation of intracellular adenylyl cyclase. The rise in intracellular cAMP acting primarily through protein kinase A (PKA) has a broad range of immunosuppressive effects.[36] Therefore, the ability to inhibit or stimulate hA_{2A} AR could be determined by evaluating their effect on cAMP production in human HEK-293 cells which stably express hA_{2A} AR.

Table 4. IC_{50} of selected compounds on cAMP assays in human HEK-293 cells[a].

Compound	hA_{2A} IC_{50} (nM)	cAMP IC_{50} (nM)
14	10.10 ± 0.98	83.00 ± 0.95
27	9.20 ± 0.97	31.00 ± 0.86
28	27.00 ± 0.99	77.00 ± 0.84

[a]Data are expressed as means ± SEM.

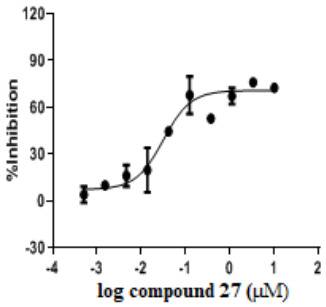

Fig. 3. The IC_{50} curve of compound 27 in cAMP functional assay.

We selected compound **14**, **27** and **28,** which show potent hA_{2A} AR binding affinity and selectivity, to assess their antagonistic activities in A_{2A} AR mediated cAMP functional assay. See Table 4 for the cyclic AMP assay results. The functional assay data for the tested compounds reflected A_{2A} AR antagonist potency. Expectedly, compound 27 with highest hA_{2A} AR antagonistic affinity (IC_{50} 9 nM of A_{2A} AR binding affinity) showed most potent functional assay data with the IC_{50} value 31 nM (Fig 3, Table 4). Compound **28** displayed less inhibition of cAMP production compared to compound **27,** consistent with its lower binding affinity to the receptor. However, compound **14** is more than 2-fold less active than compound **27** in inhibiting cAMP production despite both of these two compounds display comparable potency of A_{2A} AR binding affinity.

3.2.4. T Cell activation assay

The previous studies strongly suggested that activation of A_{2A} AR on T-cell decrease the cytokines (IL-2 and IFN-γ) production and suppress anti-tumor immune response.[17-19] In this study we examined the efficiency of A_{2A} AR antagonist compounds on T-cell activation (IL-2 production). Three compounds (**14**, **27** and **28**) were evaluated in this assay and the results are listed in Table 5. Compound **14** and **28** showed sensible activity of the IL-2 production with EC_{50} 376 nM and 555 nM respectively. It is worth noting that compound **27** shows admirable activity with EC_{50} 165 nM (Fig 4). Th1 cytokines such as IL-2 and IFN-**γ** stimulate the differentiation and activation of cytotoxic lymphocytes that are responsible for the cell-mediated immune responses against viruses and tumor cells. IL-2 is expressed by activated T cells, but not resting T cells, making it a surrogate for T-cell activation. Our compounds are able to stimulate IL-2 production by T cell activation, suggesting its potential as an immunotherapy to activate T cells for tumor killing.

Table 5. EC_{50} of selected compounds of IL-2 production on T-Cell activation[a].

Compound	hA_{2A} IC_{50} (nM)	cAMP IC_{50} (nM)	EC_{50} (nM)
14	10.10 ± 0.98	83.00 ± 0.95	376.40 ± 0.95
27	9.20 ± 0.97	31.00 ± 0.86	164.60 ± 0.34
28	27.00 ± 0.99	77.00 ± 0.84	523.60 ± 0.66

[a]Data are expressed as means ± SEM.

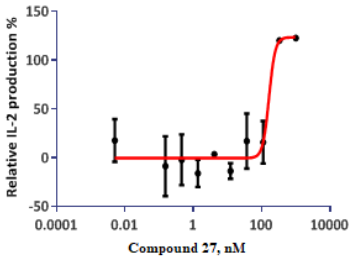

Fig. 4: The EC_{50} curve of the IL-2 production of compound 27.

3.2.5. Molecular docking studies

We performed the molecular docking modeling to interpret the hA_{2A} AR selectivity to the synthesized compound 27 at the molecular level. The binding modes of compound 27 at the hA_{2A} AR cavity were analyzed by docking simulations using the Schrodinger software (LLC, New York, NY, 2017). The docking analysis was carried out by induced fit docking module[37] associated with Glide XP algorithm[38] in Schrodinger package, and the crystal structure of hA_{2A} AR in complex with antagonist ZM241385 (PDB ID: 5NM4)[39] was used. In addition, the binding mode of hA_1 AR was also analyzed with the same docking protocols by Schrodinger.

The docking results (Fig. 5) reveal that compound 27 adopts the general binding mode[28,29,39] at both hA_{2A} AR and hA_1 AR binding sites. In this binding mode, the benzo[4,5]imidazo[1,2-a]pyrazin-1-amine scaffold positions in the depth of the binding pocket and gives π-π interaction with the Phe residue (Phe177 in hA_{2A} AR, Phe278 in hA_1 AR) (Fig. 5). In addition, the scaffold forms H-bond with the Asparagine residue in both hA_{2A} AR (Asn358) and hA_1 AR (Asn361) (Fig. 5), and it forms an additional H-bond with Glu178 in hA_{2A} AR (Fig. 5a, 5b). The substituted benzyl group is located in proximity of Leu176, Ile175, Ser76, Tyr119, Leu372, Ile379 and Met375 at the entrance of hA_{2A} AR cavity (Fig. 5a, 5b). The nonpolar profile of these cited residues at hA_{2A} AR cavity allows favorable interactions with the hydrophobic benzyl group. Whereas, the more polar profile of the corresponding hA_1 AR residues (Glu277, Ile176, Asn177, Tyr119, Ile381, His385 and Thr377) allows unfavorable interaction with the hydrophobic benzyl group (Fig. 5, c, d). Therefore, the compound 27 adopts a much more favorable binding pose at hA_{2A} AR cavity than at hA_1 AR cavity. In addition, the Glide XP docking results also indicate that the binding pose is associated with a better docking score at hA_{2A} AR (-14.14 kcal/mol) than at hA_1 AR (-11.46 kcal/mol). Hence, the molecular docking results explain the hA_{2A} AR affinity and selectivity of the compound 27.

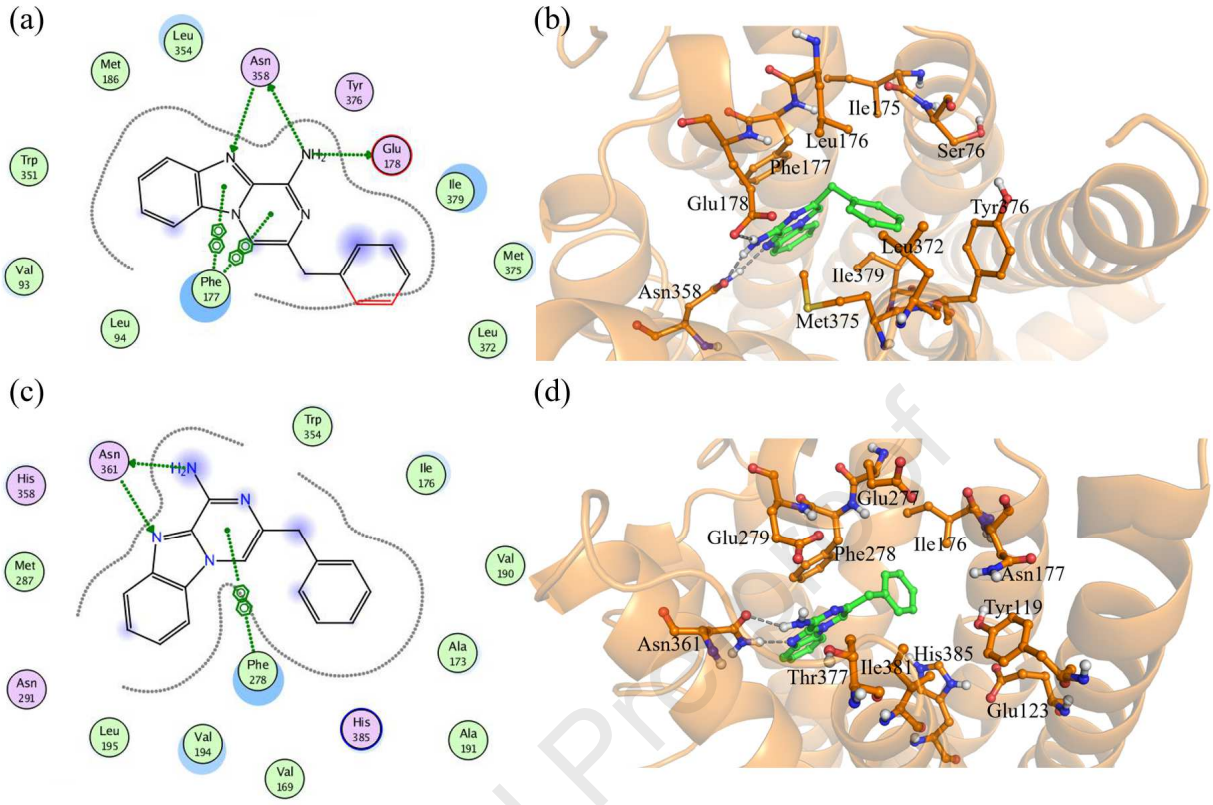

Fig. 5. Schematic description of the ligand-target interaction between compound **27** and hA_{2A} AR (a), hA_1 AR (b) (built with MOE software).[40] The binding mode of compound **27** at the hA_{2A} AR (c), hA_1 AR (d) binding cavity with indication of some key receptor residues.

4. Conclusion

In present study, we designed and synthesized a novel benzo[4,5]imidazo [1,2-*a*]pyrazin-1-amine scaffold from which a serial of derivatives were prepared and screened in sets of biological assays relevant to A_{2A} AR pathway using ZM 241385 as a benchmark reference (A_{2A} AR IC_{50} 3.9 nM, cAMP IC_{50} 5 nM, T cell activation EC_{50}, 72.3 nM), a potent and selective adenosine A_{2A} R antagonist which was widely used as a tool compound in the study of A_{2A} AR vivo biology. *In-vitro* evaluations of the A_{2A} AR, A_1 AR, cAMP and T cell assays for the synthesized compounds showed promising results. The compound **27** showed potent binding affinity to A_{2A} AR (IC_{50} 9.2 nM), good selectivity against A_1 AR (A_{2A}/A_1 80 fold) and high potency in cAMP (IC_{50} 31.0 nM) functional and IL-2 (EC_{50} 164.6 nM) production assays. With these encouraging results we anticipate that this novel benzo[4,5] imidazo[1,2-*a*]pyrazin-1-amine scaffold could be an excellent starting point for further development of A_{2A} AR antagonists to

benefit the field of cancer immunotherapy. Current effort is focused on further improving potency and selectivity against A_{2A} AR and the findings will be reported in due course.

5. Experimental section

5.1. Chemistry

All reactions were performed under mentioned conditions. Analytical thin layer chromatography was performed using TLC pre-coated silica gel 60 F_{254} (20 x 20 cm). TLC plates were visualized by exposing UV light or by iodine vapors or immersion in anisaldehyde charring reagent or in 2,4-dinitrophenyl hydrazine or ninhydrin followed by heating on hot plate. Organic solvent were concentrated by rotary evaporation and dried using high vacuum suction pump. Compounds were purified by column chromatography (flash silica gel chromatography). ^{1}H NMR spectra were recorded with 400 and 500 MHz NMR instruments. Chemical data for protons are reported in parts per million (ppm, scale) downfield from tetramethylsilane and are referenced to the residual proton in the NMR solvent ($CDCl_3$: δ 7.26, DMSO-d_6 δ 2.50 or other solvents as mentioned).

*5.1.1. General procedure for the synthesis of compounds **8-9***

*5.1.1.1. 2-(trichloromethyl)-1H-benzo[d]imidazole **(8)***

In RBF *o*-phenylenediamine (10.0 g, 92.6 mmol) was dissolved in 120 mL of AcOH. This solution was cooled to 5-10 ^oC and to this solution was added methyl 2,2,2-trichloroacetimidate drop-wise(12.48 mL, 97.23 mmol) (Note: Reaction is exothermic, so initially a few mL of methyl 2,2,2-trichloroacetimidate was added very slowly and white precipitate formed during addition). After addition the reaction was allowed to stir at room temperature for 1.5h and the reaction was monitored by TLC. After completion of the reaction, the mixture diluted with 25 mL of water and the resulting mixture was filtered. The solid cake was washed with water (3x25mL) and dried on high vacuum to give white product (19.0 g, 87%). ^{1}H NMR (DMSO-d_6, 500 MHz, δ ppm): 7.67 (2H, s), 7.34 (2H, dd, *J*=6.0, 3.1Hz); LCMS $(M+1)^+$, calculated: 236.49; found: 236.89.

*5.1.1.2. 1H-benzo[d]imidazole-2-carbonitrile **(9)***

In a sealed tube 2-(trichloromethyl)-1*H*-benzo[*d*]imidazole (5.0 g, 21.3 mmol) was taken flushed with nitrogen and cooled to 0 ^oC. 0.4 M NH_3 in dioxane (107 mL, 42.7 mmol) was added under

nitrogen slowly at 0 ^{o}C. After addition the sealed tube was closed tightly and the reaction mixture allowed stirring at room temperature for 1h. After stirring for 1h the reaction mixture was cooled to 0 ^{o}C and 7.0 M NH_3 in MeOH (6.1 mL, 42.7 mmol) was then added under nitrogen. After addition the tube was sealed tightly and the reaction mixture was allowed stirring at room temperature for 2h and reaction progress was monitored by TLC. After completion of reaction, the reaction mixture was filtered and the solid collected was then dissolved in EtOAc and water. Organic layer was separated and the aqueous layer was re-extracted with EtOAc (3x50 mL). The combined organic extracts was dried over Na_2SO_4 and concentrated. The filtrate was concentrated under reduced pressure. The resulted solid was washed with solvent mixture of ether/hexane (3/1) and ether. The solid was collected and dried on high vacuum. Yield: (2.5 g, 83 %). ^{1}H NMR (400 MHz, MeOH-d_4, δ ppm): 7.6 (2H, m), 7.4 (2H, m), LCMS $(M+H)^{+}$, calculated: 144.15; found 144.11.

*5.1.2. General procedure for the synthesis of compounds **10a-10s***

In an oven dried RBF 1*H*-benzo[*d*]imidazole-2-carbonitrile (50 mg, 0.34 mmol) was taken in dry DMF (1.5 mL). This mixture was cooled to 0 ^{o}C and K_2CO_3 (96 mg, 0.69 mmol) was added. The reaction mixture was stirred for 5 minutes and to this reaction 2-bromo-1-phenylethan-1-one (76 mg, 0.38 mmol) was then added. The reaction mixture was allowed stirring at room temperature and reaction progress was monitored by TLC. After completion of reaction, the reaction mixture was diluted with EtOAc/water. Organic layer was separated and aqueous layer was re-extracted with EtOAc (3x20 mL). The combined organic extracts was washed with brine, dried over Na_2SO_4 and concentrated. The resulted residue was chromatographed (flash silica gel chromatography) to give the desired product of 1-(2-oxo-2-phenylethyl)-1H-benzo[d]imidazole-2-carbonitrile (**10a**) with 70% yield. The synthesis, NMR data and structures of N-alkylation intermediates (**10a-10s**) is available in the supporting information section.

*5.1.3. General procedure for the synthesis of compounds **11-29**, **37-38**, **43-45**, **50***

In a sealed tube NH_4OAc(36 mg, 0.45 mmol) was added a solution of 1-(2-oxo-2-phenylethyl)-1*H*-benzo[*d*] imidazole-2-carbonitrile (40 mg, 0.15 mmol) in AcOH (1.0 mL). After addition the tube was sealed tightly and reaction mixture was allowed stirring at 90 ^{o}C and reaction progress was monitored by TLC (reaction time contrast for different substitutions). After completion of

reaction, the reaction mixture was cooled to room temperature and neutralized with saturated $NaHCO_3$ solution and extracted with EtOAc (20 mL). Organic layer was separated and aqueous layer was re-extracted with EtOAc (2x20 mL). The combined organic extracts was washed with brine, dried over Na_2SO_4 and concentrated. The resulted residue was chromatographed (flash silica gel chromatography).

5.1.3.1. 3-Phenylbenzo[4,5]imidazo[1,2-a]pyrazin-1-amine ***(11)***

Yield: (29.8 mg, 75%). ^{1}H NMR (400 MHz, DMSO-d_6, δ ppm): 8.93 (1H, s), 8.38 (1H, d, *J* = 8.1 Hz), 8.10 (2H, d, *J* = 7.7 Hz), 7.91 (1H, d, *J* = 8.1 Hz), 7.49 (7H, m). ^{13}C NMR (101 MHz, DMSO, δ ppm): 150.20, 143.56, 137.66, 135.75, 135.48, 130.36, 128.94, 128.24, 126.08, 125.98, 122.78, 120.60, 113.30, 106.32. LCMS $(M+1)^+$, calculated: 261.30, found: 261.37.

5.1.3.2. 3-(2-Methoxyphenyl)benzo[4,5]imidazo[1,2-a]pyrazin-1-amine ***(12)***

Yield: (30.3 mg, 76%). ^{1}H-NMR (500 MHz, $CDCl_3$, δ ppm): 8.49 (1H, s), 8.08 – 7.93 (2H, m), 7.87 (1H, d, *J* = 8.2 Hz), 7.54 (1H, t, *J* = 7.5 Hz), 7.37 (2H, ddd, *J* = 15.6, 11.8, 4.6 Hz), 7.15 – 6.99 (2H, m), 6.05 (2H ,s), 3.95 (3H, s). ^{13}C NMR (101 MHz, $CDCl_3$) δ 156.74, 149.08, 143.70, 135.10, 133.06, 130.55, 129.81, 129.23, 125.92, 125.76, 122.60, 121.11, 120.80, 111.48, 111.38, 110.17, 55.74. LCMS $(M+1)^+$, calculated: 291.33, found: 291.71

5.1.3.3. 3-(3-Methoxyphenyl)benzo[4,5]imidazo[1,2-a]pyrazin-1-amine ***(13)***

Yield: (29.8 mg, 75%). ^{1}H-NMR (500 MHz, DMSO-d_6, δ ppm): 8.93 (1H, s), 8.38 (1H, d, *J* = 8.1 Hz), 7.90 (1H, d, *J* = 8.2 Hz), 7.67 (2H, dd, *J* = 8.9, 5.0 Hz), 7.54 (1H, t, *J* = 7.6 Hz), 7.47 (1H, t, *J* = 7.6 Hz), 7.39 (3H, dd, *J* = 9.5, 6.2 Hz), 6.94 (1H, dd, *J* = 8.1, 2.4 Hz), 3.85 (3H, s). ^{13}C NMR (126 MHz, DMSO) δ 160.08, 150.09, 143.56, 139.14, 135.52, 130.36, 129.96, 126.00, 122.77, 120.60, 118.46, 113.70, 113.33, 111.71, 106.57, 55.64.LCMS $(M+1)^+$,calculated: 291.33, found: 291.64.

5.1.3.4. 3-(3-Bromophenyl)benzo[4,5]imidazo[1,2-a]pyrazin-1-amine ***(14)***

Yield: (27.9 mg, 70%). ^{1}H NMR (400 MHz, $CDCl_3$, δ ppm): 8.18 (1H, s), 8.13 (1H, t, *J* = 1.8 Hz), 8.02 – 7.83 (3H, m), 7.62 – 7.44 (3H, m), 7.35 (1H, t, *J* = 7.9 Hz), 5.85 (2H, s). ^{13}C NMR (126 MHz, DMSO, δ ppm): 150.20, 143.56, 140.08, 135.51, 133.98, 131.09, 130.79, 130.41,

128.58, 126.11, 124.76, 122.98, 122.66, 120.65, 113.30, 107.11. LCMS $(M+1)^+$, calculated: 339.19, found: 339.19, 341.13

5.1.3.5. 3-(p-Tolyl)benzo[4,5]imidazo[1,2-a]pyrazin-1-amine ***(15)***

Yield: (30.6 mg, 77%). ^{1}H-NMR (400 MHz, $CDCl_3$, δ ppm): 8.14 (1H, s), 8.03 – 7.78 (4H, m), 7.59 – 7.52 (1H, m), 7.45 (1H, t, *J* = 7.3 Hz), 7.29 (2H, d, *J* = 8.0 Hz), 5.90 (2H, s), 2.42 (3H, s). ^{13}C NMR (126 MHz, $CDCl_3$) δ 149.30, 143.66, 138.22, 137.01, 135.13, 134.30, 129.79, 129.54, 126.03, 126.01, 122.82, 120.95, 111.36, 105.49, 21.27. LCMS $(M+1)^+$, calculated: 275.32, found: 275.23

5.1.3.6. 3-(4-(tert-Butyl)phenyl)benzo[4,5]imidazo[1,2-a]pyrazin-1-amine ***(16)***

Yield: (28.7 mg, 72%). ^{1}H-NMR (400 MHz, $CDCl_3$, δ ppm): 8.17 (1H, s), 8.04 – 7.80 (4H, m), 7.64 – 7.43 (4H, m), 5.92 (2H, s), 1.40 (9H, s). ^{13}C NMR (126 MHz, $CDCl_3$) δ 151.47, 149.37, 143.63, 137.06, 135.14, 134.34, 129.77, 126.03, 125.91, 125.79, 122.81, 120.92, 111.36, 105.54, 34.69, 31.35. LCMS $(M+1)^+$, calculated: 317.40, found: 317.30

5.1.3.7. 3-(4-Methoxyphenyl)benzo[4,5]imidazo[1,2-a]pyrazin-1-amine ***(17)***

Yield: (31.0 mg, 78%). ^{1}H-NMR (400 MHz, $CDCl_3$, δ ppm): 8.10 (1H, s), 7.97 (1H, d, *J* = 8.3 Hz), 7.94 – 7.83 (3H, m), 7.59 – 7.53 (1H, m), 7.49 – 7.43 (1H, m), 7.05 – 6.97 (2H, m), 5.86 (2H, s), 3.88 (3H, s). ^{13}C NMR (101 MHz, $CDCl_3$) δ 159.88, 149.31, 143.52, 136.84, 134.98, 129.70, 127.41, 126.03, 122.81, 120.87, 114.22, 111.37, 104.91, 55.40. LCMS $(M+1)^+$, calculated: 291.32, found: 291.74

5.1.3.8. 4-(1-Aminobenzo[4,5]imidazo[1,2-a]pyrazin-3-yl)phenol ***(18)***

3-(4-Methoxyphenyl)benzo[4,5]imidazo[1,2-a]pyrazin-1-amine (17) 0 ± 0.20g, 0.67 mmol)) was taken up in DCM. The reaction vessel was then transferred to an ice bath and BBr_3 0 ± 0.13 mL, 38 mmol) is added slowly dropwise. After the addition is complete, the reaction mixture is allowed to stir at room temperature for 8h. After completion of the reaction, as indicated by TLC, the reaction vessel is kept un-corked, whereby the excess BBr_3 is neutralized by atmospheric moisture. It was then diluted with water and extracted with ethyl acetate. The ethyl acetate extracts are combined, dried over anhydrous Na_2SO_4, filtered and concentrated in vacuo and

column chromatographed to get the target compound, 4-(1-Aminobenzo[4,5]imidazo[1,2-a]pyrazin-3-yl)phenol (**18**) 0 ± 0.094 g, 50%). ^{1}H NMR (400 MHz, DMSO-d_6, δ ppm): 8.46 (1H, s), 8.03 (1H,s), 7.83 (2H, dd, *J* = 18.1, 8.1 Hz), 7.50 (1H, t, *J* = 7.7 Hz), 7.41 (1H, t, *J* = 8.1 Hz), 5.93 (2H, s). LCMS $(M+1)^+$, calculated: 277.29, found: 277.47.

*5.1.3.9. 3-(4-Chlorophenyl)benzo[4,5]imidazo[1,2-a]pyrazin-1-amine **(19)***

Yield: (27.9 mg, 70%)**.** ^{1}H-NMR (500 MHz, DMSO-d_6, δ ppm): 9.00 (1H, s), 8.38 (1H, d, *J* = 8.1 Hz), 8.14 (2H, d, *J* = 8.1 Hz), 7.93 (1H, d, *J* = 8.1 Hz), 7.63 – 7.42 (6H, m). ^{13}C NMR (126 MHz, DMSO) δ 150.21, 143.57, 136.57, 135.45, 134.51, 132.77, 130.37, 128.92, 127.68, 126.02, 122.88, 120.63, 113.25, 106.64. LCMS $(M+1)^+$, calculated: 295.74, found: 295.16

*5.1.3.10. 3-(4-Bromophenyl)benzo[4,5]imidazo[1,2-a]pyrazin-1-amine **(20)***

Yield: (29.5 mg, 70%). ^{1}H-NMR (400 MHz, DMSO-d_6, δ ppm): 9.00 (1H, s), 8.36 (1H, d, *J* = 8.1 Hz), 8.06 (2H, d, *J* = 8.6 Hz), 7.91 (1H, d, *J* = 8.1 Hz), 7.69 (2H, d, *J* = 8.6 Hz), 7.58 – 7.37 (4H, m). ^{13}C NMR (101 MHz, $CDCl_3$) δ 149.33, 143.63, 136.04, 135.80, 135.03, 131.91, 129.77, 127.63, 126.23, 123.11, 122.42, 121.04, 111.32, 105.91. LCMS $(M+1)^+$, calculated: 339.19, found: 339.20, 341.18.

*5.1.3.11. 3-(2,4-Difluorophenyl)benzo[4,5]imidazo[1,2-a]pyrazin-1-amine **(21)***

Yield: (25.9 mg, 65%). ^{1}H NMR (400 MHz, $CDCl_3$, δ ppm): 8.30 (1H, s), 8.09 (1H, dd, *J* = 15.8, 8.8 Hz), 7.88 (2H, dd, *J* = 25.3, 8.3 Hz), 7.45 (2H, m), 6.98 – 6.84 (2H, m), 5.76 (2H, s). LCMS $(M+1)^+$, calculated: 297.28, found: 297.21.

*5.1.3.12. 3-(4-(Trifluoromethyl)phenyl)benzo[4,5]imidazo[1,2-I]pyrazin-1-amine **(22)***

Yield: (27.9 mg, 70%). ^{1}H NMR (400 MHz, $CDCl_3$, δ ppm): 8.27 (1H, s), 8.09 (2H, d, *J* = 8.1 Hz), 8.02 (1H, d, *J* = 8.2 Hz), 7.95 (1H, d, *J* = 8.1 Hz), 7.75 (2H, d, *J* = 8.3 Hz), 7.61 (1H, t, *J* = 7.7 Hz), 7.51 (1H, t, *J* = 7.6 Hz), 5.89 (2H, s). LCMS $(M+1)^+$, calculated: 329.29, found: 329.74

*5.1.3.13. 3-(4-(Trifluoromethoxy)phenyl)benzo[4,5]imidazo[1,2-a]pyrazin-1-amine **(23)***

Yield: (29.9 mg, 75%). ^{1}H NMR (400 MHz, $CDCl_3$, δ ppm): 8.15 (1H, s), 8.10 – 7.79 (4H, m), 7.58 (1H, t, *J* = 7.7 Hz), 7.48 (1H, t, *J* = 7.7 Hz), 7.34 (2H, d, *J* = 8.3 Hz), 6.04 (2H, s). LCMS $(M+1)^+$, calculated: 345.29, found: 345.25.

5.1.3.14. 3-(4-nitrophenyl)benzo[4,5]imidazo[1,2-a]pyrazin-1-amine ***(24)***

Yield: (21.5 mg, 79%). ^{1}H NMR (400 MHz, DMSO-d_6, δ ppm): 9.21 (1 H, s), 8.41 – 8.34 (5 H, m), 7.93 (1 H, d, *J*= 8.1Hz), 7.59 – 7.48 (4 H, m). HRMS $[M+H]^+$, $C_{16}H_{11}N_5O_2$, calculated: 306.0986, found: 306.0986

5.1.3.15. 4-(1-Aminobenzo[4,5]imidazo[1,2-a]pyrazin-3-yl)benzonitrile ***(25)***

Yield: (21.6 mg, 55%). ^{1}H NMR (400 MHz, $CDCl_3$, δ ppm): 8.29 (1H, s), 8.18 – 7.90 (4H, m), 7.78 (2H, d, *J* = 8.2 Hz), 7.61 (1H, t, *J* = 7.7 Hz), 7.55 – 7.50 (1H, m), 5.89 (2H, s). LCMS $(M+1)^+$, calculated: 286.31, found: 286.22

5.1.3.16. 3-(Furan-2-yl)benzo[4,5]imidazo[1,2-a]pyrazin-1-amine ***(26)***

Yield: (27.8 mg, 70%). ^{1}H NMR (400 MHz, DMSO-d_6, δ ppm): 8.63 (1H, s), 8.37 (1H, d, *J* = 8.1 Hz), 7.90 (1H, d, *J* = 8.2 Hz), 7.78 (1H d, *J* = 0.9 Hz), 7.65 – 7.28 (4H m), 6.83 (1H, d, *J* = 3.0 Hz), 6.63 (1H, dd, *J* = 3.3, 1.8 Hz). ^{13}C NMR (126 MHz, DMSO-d_6, δ ppm): 152.65, 150.56, 143.39, 143.11, 135.40, 130.33, 129.33, 126.00, 123.02, 120.59, 113.34, 112.42, 107.46, 104.75. LCMS $(M+H)^+$, calculated: 251.26, found: 251.55.

5.1.3.17. 3-Benzylbenzo[4,5]imidazo[1,2-a]pyrazin-1-amine ***(27)***

Yield: (27.4 mg, 69%). ^{1}H NMR (400 MHz, $CDCl_3$, δ ppm): 7.94 (1H. d, *J* = 8.3 Hz), 7.75 (1H, d, *J* = 8.3 Hz), 7.52 (2H, dd, *J* = 11.7, 4.5 Hz), 7.44 – 7.25 (6H, m), 5.83 (2H, s), 4.01 (2H, s). ^{13}C NMR (101 MHz, $CDCl_3$, δ ppm): 149.64, 143.41, 138.72, 138.35, 134.92, 129.49, 129.19, 128.67, 126.69, 125.81, 122.70, 120.80, 111.32, 107.18, 41.13. LCMS $(M+1)^+$, calculated: 275.32, found: 275.66

5.1.3.18. 7,8-Difluoro-3-(3-methoxyphenyl)benzo[4,5]imidazo[1,2-a]pyrazin-1-amine ***(28)***

Yield: (21.9 mg, 55%). ^{1}H NMR (400 MHz, $CDCl_3$, δ ppm): 8.03 (1H, s), 7.71 (2H, m), 7.48 (2H, dd, *J* = 9.7, 5.0 Hz), 7.39 (1H, t, *J* = 7.9 Hz), 6.95 (1H, dd, *J* = 8.1, 2.5 Hz), 5.84 (2H s), 3.91 (3H

s). ^{13}C NMR (126 MHz, $CDCl_3$) δ 160.14, 148.92, 138.21, 137.41, 129.87, 118.36, 114.21, 111.88, 107.96, 107.80, 105.66, 99.29, 99.11, 55.42. LCMS $(M+1)^+$, calculated: 327.30, found: 327.26

5.1.3.19. 4-Methyl-3-phenylbenzo[4,5]imidazo[1,2-a]pyrazin-1-amine ***(29)***

Yield: (25.9 mg, 65%). ^{1}H NMR (500 MHz, $CDCl_3$, δ ppm): 8.12 (1H, d, *J* = 8.5 Hz), 7.94 (1H, d, *J* = 8.3 Hz), 7.52 – 7.44 (3H, m), 7.41 (2H, t, *J* = 7.5 Hz), 7.33 (2H, t, *J* = 7.6 Hz), 5.72 (2H, s), 2.86 (3H s). ^{13}C NMR (101 MHz, $CDCl_3$, δ ppm): 147.86, 143.98, 138.71, 136.04, 135.48, 131.39, 129.86, 128.37, 127.87, 125.38, 122.62, 120.88, 119.50, 115.10, 17.23. LCMS $(M+1)^+$, calculated: 275.32, found: 275.45.

5.1.3.20. N-(4-(1-aminobenzo[4,5]imidazo[1,2-a]pyrazin-3-yl)phenyl)acetamide ***(37)***

^{1}H NMR (400 MHz, DMSO-d_6, δ ppm): 10.05 (1 H, s), 8.85 (1 H, s), 8.35 (1 H, d, *J* =8.1Hz), 8.01 (2 H, d, *J*= 8.7Hz), 7.90 (1 H, d, *J* =8.1Hz), 7.69 (2 H, d, *J* =8.7Hz), 7.53 (1 H, t, *J* =7.6Hz), 7.46 (1 H, t, *J*= 7.6Hz), 7.36 (2 H, s), 2.08 (3 H, s). HRMS $[M+H]^+$, $C_{18}H_{15}N_5O$, calculated: 318.1349, found: 318.1346

5.1.3.21. N-(3-(1-aminobenzo[4,5]imidazo[1,2-a]pyrazin-3-yl)phenyl)acetamide ***(38)***

^{1}H NMR (500 MHz, DMSO-d_6, δ ppm): 10.07 (1 H, s), 8.82 (1 H, s), 8.37 (1 H, d, *J*=8.2 Hz), 8.18 (1 H, s), 7.91 (1 H, d, *J*= 8.2 Hz), 7.71 (1 H, d, *J*= 7.8 Hz), 7.62 (1 H, d, *J* =7.9 Hz), 7.54 (1 H, t, *J*= 7.6 Hz), 7.47 (1 H, t, *J* =7.6 Hz), 7.42 – 7.33 (3 H, m), 2.08 (3 H, s). LCMS $(M+Na)^+$, calculated: 340.34, found: 340.50

5.1.3.22. 3-(piperidin-4-yl)benzo[4,5]imidazo[1,2-a]pyrazin-1-amine ***(43)***

^{1}H NMR (500 MHz, MeOD, δ ppm): 8.07 (1 H, d, *J* =8.3 Hz), 7.95 (1 H, s), 7.86 (1 H, d, *J*= 8.3 Hz), 7.54 (1 H, t, *J* =7.7 Hz), 7.45 (1 H, t, *J* =7.7 Hz), 3.26 (2 H, d, *J* =12.5 Hz), 2.84 (2 H, t, *J* =12.4 Hz), 2.78 – 2.70 (1 H, m), 2.04 (2 H, d, *J* =13.0 Hz), 1.89 – 1.78 (2 H, m). HRMS $[M+H]^+$, $C_{15}H_{17}N_5$, calculated: 268.1557, found: 268.1559

5.1.3.23. 3-(1-(2-methoxyethyl)piperidin-4-yl)benzo[4,5]imidazo[1,2-a]pyrazin-1-amine ***(44)***

^{1}H NMR (400 MHz, MeOD, δ ppm): 8.05 (1 H, d, *J*= 8.3), 7.92 (1 H, s), 7.84 (1 H, d, *J*= 8.3 Hz), 7.54 – 7.49 (1 H, m), 7.45 – 7.40 (1 H, m), 3.60 (2 H, t, *J* =5.6 Hz), 3.37 (3 H, s), 3.21 (2 H, d, *J*= 12.0 Hz), 2.75 (2 H, t, *J* =5.6 Hz), 2.65 – 2.54 (1 H, m), 2.35 (2 H, td, *J*= 12.0, 2.2 Hz), 2.06 – 1.99 (2 H, m), 1.98 – 1.86 (2 H, m). HRMS $[M+H]^+$, $C_{18}H_{23}N_5O$, calculated: 326.1975, found: 326.1972

5.1.3.24. 2-(4-(1-aminobenzo[4,5]imidazo[1,2-a]pyrazin-3-yl)piperidin-1-yl)-1-morpholinoethan-1-one ***(45)***

^{1}H NMR (500 MHz, $CDCl_3$, δ ppm): 7.95 (1 H, d, *J*=8.1 Hz), 7.83 (1 H, d, *J* =8.2 Hz), 7.60 (1 H, s), 7.53 (1 H, t, *J*= 7.5 Hz), 7.43 (1 H, t, *J* =7.4 Hz), 5.73 (2 H, s), 3.76 – 3.60 (7 H, m), 3.26 (2 H, s), 3.05 (2 H, d, *J* =10.3 Hz), 2.56 (1 H, t, *J* =11.6 Hz), 2.34 – 2.19 (2 H, m), 2.04 (2 H, d, *J*= 12.3 Hz), 1.91 – 1.79 (2 H, m). HRMS $[M+H]^+$, $C_{21}H_{26}N_6O_2$, calculated: 395.2190, found: 395.2188.

5.1.3.25. (1-aminobenzo[4,5]imidazo[1,2-a]pyrazin-3-yl)methanol ***(50)***

^{1}H NMR (400 MHz, DMSO) δ 8.24 (1H, d, *J* = 8.2 Hz), 8.14 (1H, s), 7.87 (1H, d, *J* = 8.2 Hz), 7.54 – 7.47 (1H, m), 7.45 – 7.39 (1H, m), 7.23 (2H, s), 5.32 (1H, s), 4.45 (2H, s). HRMS $[M+H]^+$, $C_{11}H_{10}N_4O$, calculated: 215.0927, found: 215.0929.

5.2. Biological activity

5.2.1. A_{2A} AR binding assay

The synthesized compounds were tested to evaluate their affinity for the A_{2A} AR expressed on HEK293 cell membranes. The assay buffer (50 mM Tris-HCl of pH 7.4; 10 mM $MgCl_2$; 1 mM EDTA; 1 μg/mL adenosine deaminase) was prepared and stored at 4˚C for use. The wash buffer (50 mM Tris-HCl of pH 7.4; 154 mM NaCl) was prepared and stored at 4˚C for use. 0.5% PEI solution was prepared by dissolving 0.5 g of PEI in 100 mL of ddH_2O and stored at 4˚C for use. 1 μL Of A_{2A} membrane (hA_{2A} HEK-293 membrane) and 300 μL of assay buffer was added into 96-well plate in which each well contains testing compound (10 different concentrations from 1000 nM to 0.05 nM by three-fold sequential dilution) and the plate was shaken for 5 minutes. [^{3}H]-ZM241385 (final concentration 0.5 nM) was then added to the assay well and the plate was incubated for 1.5h at 27 ^{o}C. Bound radioactivity and free radioactivity were separated by filtering

the assay mixture through a UNIFILTER-96 GF/B filter plate (pre-incubated with 0.5% PEI for 1 h) and washed with wash buffer. ULTIMA GOLD (40 µL) was added to each well of the plate and the count per minute (CPM) was read on TopCount.

5.2.2. A_1 AR binding assay

The synthesized compounds were tested to evaluate their affinity for the A_1 AR expressed on CHO-K1 cell membranes. The assay buffer (50 mM Tris-HCl of pH 7.4; 10 mM $MgCl_2$; 1 mM EDTA; 1 µg/mL adenosine deaminase) was prepared and stored at 4˚C for use. The wash buffer was prepared and stored at 4˚C for use. 0.5% PEI solution was prepared by dissolving 0.5 g of PEI in 100 mL of ddH_2O and stored at 4˚C for use. The CHO-K1 cells with adenosine A_1 (human) membrane were purchased from Perkinelmer. The dilution of A_1 membrane (hA_1 CHO-K1 membrane) was performed by dissolving 20 U of A_1 membrane and 0.41 uCi [^{3}H] DPCPX (final concentration 2.5 nM) in 1 mL of assay buffer. 50 µL of diluted A_1 membrane was then added into 96-well plate in which each well contains testing compound (10 different concentrations from 1000 nM to 0.05 nM by three-fold sequential dilution) and the plate was shaken for 5 minutes. The plate was then incubated at 25 ˚C for 50 minutes. The membrane mixture was filtered through UNIFILTER-96 GF/B filter plate (pre-incubated with 0.5% of PEI at 4˚C for 1.5 hours and then washed twice with 1 mL of wash buffer per well) and washed four times (4x500 µL for each well) with wash buffer. After the plate was dried at 55˚C for 10 minutes, 40 µL of ULTIMA GOLD was added to each well and the CPM was recorded by TopCount.

5.2.3. Cyclic AMP functional assay

HEK293-A_{2A} cells which express human A_{2A} AR were cultured in a growth medium [this medium contains DMEM (Gibco), 10% FBS (Gibco), 1X Penicillin-Streptomycin (Gibco), and 400µg/mL of G418 (Invitrogen)] at 37 °C under 5% CO_2. The assay buffer in which contains 1xHBSS, 0.1% BSA (Perkin Elmer), 20mM HEPES (Gibco) and 100nM IBMX (Sigma) was prepared and stored at room temperature for assay use. The 8x test compound stock solution and 8x NECA stock solution (12 nM) were prepared with assay buffer for use. 20X cAMP-d2 and 20X anti-cAMP-Eu3+ detection reagent solutions were prepared using lysis buffer. Briefly, HEK293-A_{2A} cells were seeded in 384-well plate (6007680-50, PE) in which each well contains

15,000 cells suspended in 15 μL of assay buffer. 2.5μL of test compound solution was added to indicated well of the 384-well plate prepared above and incubated at 37 °C for 10 minutes. Next, 2.5μL of NECA stock solution was added to the 384-well plate and incubated at 37 °C for additional 30 minutes (the final volume of the reaction system is 20μL). Finally, 10μL of cAMP-d2 and 10μL of anti-cAMP-Eu3+ detection reagent were added into each well of the plate and incubated at room temperature for 1h. The data was collected at the wavelength of 665 nm and 615 nm on Envision 2104 plate reader.

5.2.4. T-cell activation assay

T cells were isolated using Human Pan T Cell Isolation Kit (MicroBead No. 130-096-535) from fresh human peripheral blood mononuclear cells (Sailybio, No. SLB-HP100A). The human pan T cell was seeded into the 96-well plate and incubated at 37 °C under 5% CO_2 for 1 hour. To the cells 2μL of NECA and 2μL of test compound (final concentration of DMSO is 0.2%) were added and the cells were incubated at 37 °C under 5% CO_2 for 1 hour. T cells were treated by adding 5μL of dynabeads of human T-activator CD3/CD28 (Gibcono. No.11131D) for T cell expansion and activation and then incubated at 37°C under 5% CO_2 for 1 hour. The plate was centrifuged and the supernatant was transferred into another 96-well plate which was assayed for IL-2 production using human IL-2 Quantikine ELISA Kit (R&D, No. D2050). Data were collected and analyzed with Read Abs450 on envision.

5.3. Molecular docking

The crystal structure of hA_{2A} AR in complex with antagonist ZM241385 (PDB ID: 5NM4)[41] was downloaded from Protein Data Bank (http://www.pdb.org), and the structure of hA_1 R in complex with antagonist PSB36 (PDB ID: 5N2S)[41] was also retrieved. The crystal structures of hA_{2A} AR and hA_1 AR were remodeled by first removing the antagonists from the protein and second adding the missing residues and atoms using SWISS-MODEL.[42] Then the hydrogen atoms and disulfide bonds of the proteins were added by AmerTools to prepare the initial structures for molecular docking.

The molecular dockings were carried out by Schrodinger software (LLC, New York, NY, 2017). The proteins and ligand preparations for docking were performed by Maestro (Schrödinger). The proteins were prepared using the Protein Preparation Wizard, and the ligand was treated by

OPLS2005 force field. The induced fit Glide docking program[37] that considering the conformational changes of the protein was used for docking studies. For the Glide docking, the grid was defined using the auto-size box centered on residue Met365 of hA_{2A} AR and Thr377 of hA_1 AR respectively. The protein preparation constrained refinement was selected, and the side-chain trimming procedure as well as VDW scaling was used to create more room for the ligand in the active site. The compound **27** was docked using Glide XP mode.[38,43] and the predicted binding modes in hA_{2A} AR and hA_1 AR were ranked according to their glide scores.

Acknowledgements

Financial support from the National Natural Science Fundation of China (21772043, **82003651**) is greatly acknowledged. We also are thankful for the financial support from Guangdong Innovative and Entrepreneurial Research Team Program (No. 2016ZT06Y337) and the Fundamental Research Funds for the Central Universities (#19ykpy135, **#20ykpy113, No31143408**)

Appendix. Supplementary data

Supplementary data associated with this article can be found in the online version.

Reference

[1] B.B. Fredholm, A.P. IJzerman, K.A. Jacobson, J. Linden, C.E. Müller, International Union of Basic and Clinical Pharmacology. LXXXI. Nomenclature and Classification of Adenosine Receptors—An Update, Pharmacol. Rev. 63 (2011) 1-34.

[2] D. Dal Ben, C. Lambertucci, S. Vittori, R. Volpini, G. Cristalli, GPCRs as therapeutic targets: a view on adenosine receptors structure and functions, and molecular modeling support, Journal of the Iranian Chemical Society. 2 (2005) 176-188.

[3] D. Vijayan, A. Young, M.W. Teng, M.J. Smyth, Targeting immunosuppressive adenosine in cancer, Nature Reviews Cancer. 17 (2017) 709-724.

[4] A.M. Almerico, M. Tutone, L. Pantano, A. Lauria, A3 adenosine receptor: Homology modeling and 3D-QSAR studies, J. Mol. Graph. Model. 42 (2013) 60-72.

[5] A. Guerrero, A2A adenosine receptor agonists and their potential therapeutic applications. An update, Curr. Med. Chem. 25 (2018) 3597-3612.

[6] M.V. Sitkovsky, D. Lukashev, S. Apasov, H. Kojima, M. Koshiba, C. Caldwell, A. Ohta, M. Thiel, Physiological control of immune response and inflammatory tissue damage by hypoxia-inducible factors and adenosine A2A receptors, Annu. Rev. Immunol. 22 (2004) 657-682.

[7] M. de Lera Ruiz, Y.-H. Lim, J. Zheng, Adenosine A2A receptor as a drug discovery target, J. Med. Chem. 57 (2014) 3623-3650.

[8] M. Congreve, G.A. Brown, A. Borodovsky, M.L. Lamb, Targeting adenosine A2A receptor antagonism for treatment of cancer, Expert Opinion on Drug Discovery. 13 (2018) 997-1003.

[9] M. Zhang, S. Fan, X. Zhou, F. Xie, S. Li, W. Zhong, Design, synthesis and biological evaluation of 2-hydrazinyladenosine derivatives as A2A adenosine receptor ligands, Eur. J. Med. Chem. 179 (2019) 310-324.

[10] D. Preti, P.G. Baraldi, G. Saponaro, R. Romagnoli, M. Aghazadeh Tabrizi, S. Baraldi, S. Cosconati, A. Bruno, E. Novellino, F. Vincenzi, Design, Synthesis, and Biological Evaluation of Novel 2-((2-(4-(Substituted) phenylpiperazin-1-yl) ethyl) amino)-5′-N-ethylcarboxamidoadenosines as Potent and Selective Agonists of the A2A Adenosine Receptor, J. Med. Chem. 58 (2015) 3253-3267.

[11] S. Morello, R. Sorrentino, A. Pinto, Adenosine A2a receptor agonists as regulators of inflammation: pharmacology and therapeutic opportunities, Journal of Receptor, Ligand and Channel Research. 2 (2009) 11-17.

[12] C.M. Lappas, G.W. Sullivan, J. Linden, Adenosine A2A agonists in development for the treatment of inflammation, Expert opinion on investigational drugs. 14 (2005) 797-806.

[13] R. Franco, G. Navarro, Adenosine A2A receptor antagonists in neurodegenerative diseases: Huge potential and huge challenges, Frontiers in psychiatry. 9 (2018) 68.

[14] M.R. Domenici, A. Ferrante, A. Martire, V. Chiodi, R. Pepponi, M.T. Tebano, P. Popoli, Adenosine A2A receptor as potential therapeutic target in neuropsychiatric disorders, Pharmacol. Res. 147 (2019) 104338.

[15] O.H. Al-Attraqchi, M. Attimarad, K.N. Venugopala, A. Nair, N.H. Al-Attraqchi, Adenosine A2A receptor as a potential drug target-current status and future perspectives, Curr. Pharm. Des. 25 (2019) 2716-2740.

[16] J. Zheng, X. Zhang, X. Zhen, Development of adenosine A2A receptor antagonists for the treatment of Parkinson's disease: a recent update and challenge, ACS Chem. Neurosci. 10 (2018) 783-791.

[17] K. Sek, C. Mølck, G.D. Stewart, L. Kats, P.K. Darcy, P.A. Beavis, Targeting adenosine receptor signaling in cancer immunotherapy, Int. J. Mol. Sci. 19 (2018) 3837.

[18] S. Merighi, E. Battistello, L. Giacomelli, K. Varani, F. Vincenzi, P.A. Borea, S. Gessi, Targeting A3 and A2A adenosine receptors in the fight against cancer, Expert Opin. Ther. Targets. 23 (2019) 669-678.

[19] A. Young, S.F. Ngiow, Y. Gao, A.-M. Patch, D.S. Barkauskas, M. Messaoudene, G. Lin, J.D. Coudert, K.A. Stannard, L. Zitvogel, A2AR adenosine signaling suppresses natural killer cell maturation in the tumor microenvironment, Cancer Res. 78 (2018) 1003-1016.

[20] R.D. Leone, Y.-C. Lo, J.D. Powell, A2aR antagonists: Next generation checkpoint blockade for cancer immunotherapy, Computational and structural biotechnology journal. 13 (2015) 265-272.

[21] A.T. Waickman, A. Alme, L. Senaldi, P.E. Zarek, M. Horton, J.D. Powell, Enhancement of tumor immunotherapy by deletion of the A 2A adenosine receptor, Cancer Immunology, Immunotherapy. 61 (2012) 917-926.

[22] S.B. Willingham, P.Y. Ho, A. Hotson, C. Hill, E.C. Piccione, J. Hsieh, L. Liu, J.J. Buggy, I. McCaffery, R.A. Miller, A2AR antagonism with CPI-444 induces antitumor responses and augments efficacy to anti–PD-(L) 1 and anti–CTLA-4 in preclinical models, Cancer immunology research. 6 (2018) 1136-1149.

[23] P.A. Beavis, U. Divisekera, C. Paget, M.T. Chow, L.B. John, C. Devaud, K. Dwyer, J. Stagg, M.J. Smyth, P.K. Darcy, Blockade of A2A receptors potently suppresses the metastasis of CD73+ tumors, Proceedings of the National Academy of Sciences. 110 (2013) 14711-14716.

[24] A. Ohta, E. Gorelik, S.J. Prasad, F. Ronchese, D. Lukashev, M.K. Wong, X. Huang, S. Caldwell, K. Liu, P. Smith, A2A adenosine receptor protects tumors from antitumor T cells, Proceedings of the National Academy of Sciences. 103 (2006) 13132-13137.

[25] W.G. Kerr, J.D. Chisholm, The next generation of immunotherapy for cancer: small molecules could make big waves, The Journal of Immunology. 202 (2019) 11-19.

[26] A. Young, S.F. Ngiow, D.S. Barkauskas, E. Sult, C. Hay, S.J. Blake, Q. Huang, J. Liu, K. Takeda, M.W. Teng, Co-inhibition of CD73 and A2AR adenosine signaling improves anti-tumor immune responses, Cancer Cell. 30 (2016) 391-403.

[27] R.D. Leone, L.A. Emens, Targeting adenosine for cancer immunotherapy, Journal for immunotherapy of cancer. 6 (2018) 57.

[28] M. Falsini, D. Catarzi, F. Varano, C. Ceni, D. Dal Ben, G. Marucci, M. Buccioni, R. Volpini, L. Di Cesare Mannelli, E. Lucarini, Antioxidant-conjugated 1, 2, 4-triazolo [4, 3-a] pyrazin-3-one derivatives: highly potent and selective human A2A adenosine receptor antagonists possessing protective efficacy in neuropathic pain, J. Med. Chem. 62 (2019) 8511-8531.

[29] M. Falsini, L. Squarcialupi, D. Catarzi, F. Varano, M. Betti, D. Dal Ben, G. Marucci, M. Buccioni, R. Volpini, T. De Vita, The 1, 2, 4-triazolo [4, 3-a] pyrazin-3-one as a versatile scaffold for the design of potent adenosine human receptor antagonists. Structural investigations to target the A2A receptor subtype, J. Med. Chem. 60 (2017) 5772-5790.

[30] D. Poli, M. Falsini, F. Varano, M. Betti, K. Varani, F. Vincenzi, A.M. Pugliese, F. Pedata, D. Dal Ben, A. Thomas, Imidazo [1, 2-a] pyrazin-8-amine core for the design of new adenosine receptor antagonists: Structural exploration to target the A3 and A2A subtypes, Eur. J. Med. Chem. 125 (2017) 611-628.

[31] H. Peng, G. Kumaravel, G. Yao, L. Sha, J. Wang, H. Van Vlijmen, T. Bohnert, C. Huang, C.B. Vu, C.L. Ensinger, Novel bicyclic piperazine derivatives of triazolotriazine and triazolopyrimidines as highly potent and selective adenosine A2A receptor antagonists, J. Med. Chem. 47 (2004) 6218-6229.

[32] G. Yao, S. Haque, L. Sha, G. Kumaravel, J. Wang, T.M. Engber, E.T. Whalley, P.R. Conlon, H. Chang, W.F. Kiesman, Synthesis of alkyne derivatives of a novel triazolopyrazine as A2A adenosine receptor antagonists, Bioorg. Med. Chem. Lett. 15 (2005) 511-515.

[33] R. Goel, V. Luxami, K. Paul, Recent advances in development of imidazo [1, 2-a] pyrazines: synthesis, reactivity and their biological applications, Org. Biomol. Chem. 13 (2015) 3525-3555.

[34] J.D. Venable, H. Cai, W. Chai, C.A. Dvorak, C.A. Grice, J.A. Jablonowski, C.R. Shah, A.K. Kwok, K.S. Ly, B. Pio, Preparation and biological evaluation of indole, benzimidazole, and

thienopyrrole piperazine carboxamides: potent human histamine H4 antagonists, J. Med. Chem. 48 (2005) 8289-8298.

[35] L. Garuti, M. Roberti, A. Pession, E. Leoncini, S. Hrelia, Synthesis and antiproliferative activity of some thiazolylbenzimidazole-4, 7-diones, Bioorg. Med. Chem. Lett. 11 (2001) 3147-3149.

[36] T. Raskovalova, A. Lokshin, X. Huang, Y. Su, M. Mandic, H.M. Zarour, E.K. Jackson, E. Gorelik, Inhibition of cytokine production and cytotoxic activity of human antimelanoma specific CD8+ and CD4+ T lymphocytes by adenosine-protein kinase A type I signaling, Cancer Res. 67 (2007) 5949-5956.

[37] O. Kalid, D.T. Warshaviak, S. Shechter, W. Sherman, S. Shacham, Consensus Induced Fit Docking (cIFD): methodology, validation, and application to the discovery of novel Crm1 inhibitors, Journal of computer-aided molecular design. 26 (2012) 1217-1228.

[38] R.A. Friesner, R.B. Murphy, M.P. Repasky, L.L. Frye, J.R. Greenwood, T.A. Halgren, P.C. Sanschagrin, D.T. Mainz, Extra precision glide: Docking and scoring incorporating a model of hydrophobic enclosure for protein− ligand complexes, J. Med. Chem. 49 (2006) 6177-6196.

[39] T. Weinert, N. Olieric, R. Cheng, S. Brünle, D. James, D. Ozerov, D. Gashi, L. Vera, M. Marsh, K. Jaeger, Serial millisecond crystallography for routine room-temperature structure determination at synchrotrons, Nature communications. 8 (2017) 1-11.

[40] Molecular Operating Environment, in, C.C.G. Inc., 1255 University St., Suite 1600, Montreal, Quebec, Canada.

[41] R.K. Cheng, E. Segala, N. Robertson, F. Deflorian, A.S. Doré, J.C. Errey, C. Fiez-Vandal, F.H. Marshall, R.M. Cooke, Structures of human A1 and A2A adenosine receptors with xanthines reveal determinants of selectivity, Structure. 25 (2017) 1275-1285. e1274.

[42] A. Waterhouse, M. Bertoni, S. Bienert, G. Studer, G. Tauriello, R. Gumienny, F.T. Heer, T.A.P. de Beer, C. Rempfer, L. Bordoli, SWISS-MODEL: homology modelling of protein structures and complexes, Nucleic Acids Res. 46 (2018) W296-W303.

[43] R.A. Friesner, J.L. Banks, R.B. Murphy, T.A. Halgren, J.J. Klicic, D.T. Mainz, M.P. Repasky, E.H. Knoll, M. Shelley, J.K. Perry, Glide: a new approach for rapid, accurate docking and scoring. 1. Method and assessment of docking accuracy, J. Med. Chem. 47 (2004) 1739-1749.

Highlights

Design, synthesis and biological evaluation of novel scaffold benzo[4,5]imidazo[1,2-*a*]pyrazin-1-amine: towards adenosine A_{2A} receptor (A_{2A} AR) antagonist

G. Lakshma Reddy, Rupam Sarma, Shuhao Liu, Weifeng Huang, Jinping Lei,* Jiasheng Fu,* Wenhao Hu*

Highlights

- Design new benzo[4,5]imidazo[1,2-a]pyrazin-1-amine scaffold
- Developed simple protocol for the synthesis of benzo[4,5]imidazo[1,2-a]pyrazin-1-amine scaffold analogues
- This new analogues biological evaluated for Adenosine A_{2A} receptor (A_{2A}) antagonist activety
- cAMP Functional assays of the hA_{2A} AR in human HEK-293 cells, compound **27** showed nonomolar potency with IC_{50}= 31 nM
- Compound **27** stimulate IL-2 production by T cell activation with nonomolar potency i.e. EC_{50} = 165 nM

Declaration of interests

☒ The authors declare that they have no known competing financial interests or personal relationships that could have appeared to influence the work reported in this paper.

☐The authors declare the following financial interests/personal relationships which may be considered as potential competing interests: